Maximizing the Giant Liquid Slip on Superhydrophobic Microstructures by Nanostructuring Their Sidewalls

ARTICLE *in* LANGMUIR · AUGUST 2009

Impact Factor: 4.46 · DOI: 10.1021/la901824d · Source: PubMed

2 AUTHORS:

Choongyeop Lee
Kyung Hee University
18 PUBLICATIONS **443** CITATIONS
SEE PROFILE

Chang-Jin Kim
University of California, Los Angeles
256 PUBLICATIONS **7,949** CITATIONS
SEE PROFILE

Langmuir
Article
pubs.acs.org/Langmuir

Maximizing the Giant Liquid Slip on Superhydrophobic Microstructures by Nanostructuring Their Sidewalls

Choongyeop Lee* and Chang-Jin "CJ" Kim

Mechanical and Aerospace Engineering Department, University of California, Los Angeles (UCLA), Los Angeles, California 90034

Received May 21, 2009. Revised Manuscript Received July 1, 2009

In an effort to maximize the liquid slip on superhydrophobic surfaces, we investigate the role of the nanoscale roughness on microscale structures by developing well-defined micro−nano hierarchical structures. The nonwetting stability and slip length on the dual-scale micro−nano structures are measured and compared with those on single-scale micro-smooth structures. A force balance between a liquid pressure and a surface tension indicates that hydrophobic nanostructures on the sidewall of microposts or microgrates would expand the range of the nonwetted state. When a higher gas fraction or a larger pitch can be tested without wetting, a larger slip length is expected on the microstructures. An ideal dual-scale structure is described that isolates the role of the nanostructures, and a fabrication technique is developed to achieve such a microstructure—smooth tops and nanostructured sidewalls. The tests confirm such micro−nano structures allow a nonwetted state at a higher gas fraction or a larger pitch than the previous micro-smooth structures. As a result, we achieve the maximum slip length of ~400 μm on the dual-scale structures, an increase of ~100% over the previous maximum reported on the single-scale (i.e., micro-smooth) structures. The study ameliorates our understanding of the role of each scale on hierarchical structures for a wetting transition and a liquid slip. The resulting giant slip is large enough to influence many fluidic applications, even in macroscale.

Introduction

It is well understood that an effective liquid slip can be generated on a structured hydrophobic surface, such as Nanoturf,[1] due to the presence of gas in between the structures. While a true slip on smooth surfaces has been too small (e.g., nanometers) for any meaningful usage, an effective slip on a structured hydrophobic surface is large enough (e.g., micrometers) to consider several potential applications, such as amplification of diffusion osmosis[2] and friction drag reduction for both laminar[3−5] and turbulent[6] flows. However, the influence of a liquid slip is pronounced only if the length scale of the fluidic system is comparable to a slip length, which is defined as the virtual distance from the top surface into to the wall where a liquid velocity vanishes to zero by a linear extrapolation.[4]

The slip length reported on most superhydrophobic surfaces ranged from hundreds of nanometers to tens of micrometers[3−5,7] until recent years. In an effort to obtain a slippage large enough to affect regular or macroscale fluidic applications (for example, a giant slip length over 100 μm), a systematic parametric study of surface geometries' influence on the slip length was carried out experimentally. The results confirmed that the key for such a large slip was to maximize a gas fraction or a pitch of the microstructure that would stay nonwetted.[8] Once a meniscus lost its stability by the liquid pressure, the structured surface transitioned from a nonwetted state (Figure 1a) to a (either partially or fully) wetted state (Figure 1b), negating virtually all of the gained slip. In the range of giant slips, this transition from a nonwetted to a wetted state, which we will call a wetting transition, is a primary event delimiting the maximum achievable slip length for a given flow condition. To increase the maximum, therefore, one would have to control the wetting transition. Recently, it was shown that a wetting transition could be delayed to a higher liquid pressure by pressurizing an inside air layer both actively[9] and passively.[10] However, both of the approaches required an additional energy input or complex configurations, making it difficult to extend to an area larger than for microscale applications.

There also have been several investigations into fundamental aspects of various wetting transition mechanisms experimentally[11,12] and analytically.[13,14] Although most of the studies were based on a liquid droplet, their main findings can be useful for the continuous liquid flows as well. In particular, it was theoretically contemplated how hierarchical structures would affect a wetting transition by calculating the evolution of thermodynamic energy during a wetting transition.[14] According to the calculation, a local energy minimum can be created by imposing small bumps over pillars in the path of a wetting transition. A liquid−gas meniscus is likely to be pinned at the location of the local energy minimum even with the presence of surface inhomogeneity, rendering a superhydrophobic surface more robust to a

*Corresponding author: Tel 1-310-825-3977; Fax 1-310-206-2302; e-mail choongyeop@ucla.edu.

(1) Kim, J.; Kim, C.-J. *Proceedings of the 15th IEEE International Conference on Micro Electro Mechanical Systems*; IEEE: Piscataway, 2002; pp 479−482.
(2) Huang, D. M.; Cottin-Bizonne, C.; Ybert, C.; Bocquet, L. *Phys. Rev. Lett.* **2008**, *101*, 064503.
(3) Ou, J.; Perot, B.; Rothstein, J. P. *Phys. Fluids* **2004**, *16*, 4635–4643.
(4) Choi, C.-H.; Kim, C.-J. *Phys. Rev. Lett.* **2006**, *96*, 066001.
(5) Choi, C.-H.; Ulmanella, U.; Ho, C.-M.; Kim, C.-J. *Phys. Fluids* **2006**, *18*, 087105.
(6) Martell, M. B.; Perot, J. B.; Rothstein, J. P. *J. Fluid Mech.* **2009**, *620*, 31–41.
(7) Joseph, P.; Cottin-Bizonne, C.; Benoit, J.-M.; Ybert, C.; Journet, C.; Tabeling, P.; Bocquet, L. *Phys. Rev. Lett.* **2006**, *97*, 156104.
(8) Lee, C.; Choi, C.-H.; Kim, C.-J. *Phys. Rev. Lett.* **2008**, *101*, 064501.
(9) Carlborg, C. F.; Do-Quang, M.; Stemme, G.; Amberg, G.; van der Wijngaart, W. *Proceedings of the 21th IEEE International Conference on Micro Electro Mechanical Systems*; IEEE: Tucson, 2008; pp 599−602.
(10) Carlborg, C. F.; Stemme, G.; van der Wijngaart, W. *Proceedings of the 22th IEEE International Conference on Micro Electro Mechanical Systems*; IEEE: Sorrento, 2009; pp 39−42.
(11) Lafuma, A.; Quere, D. *Nat. Mater.* **2003**, *2*, 457–460.
(12) Nosonovsky, M.; Bhushan, B. *Langmuir* **2008**, *24*, 1525–1533.
(13) Zheng, Q.-S.; Yu, Y.; Zhao, Z.-H. *Langmuir* **2005**, *21*, 12207–12212.
(14) Nosonovsky, M.; Bhushan, B. *Ultramicroscopy* **2007**, *107*, 969–979.

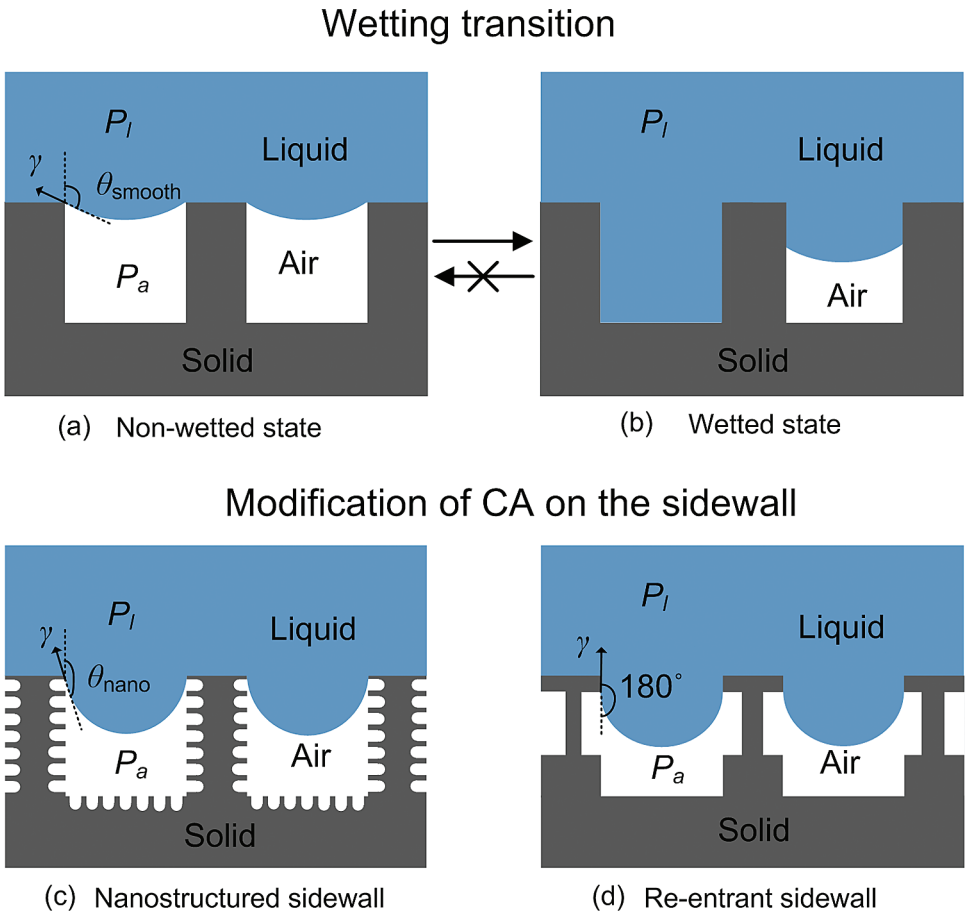

Figure 1. Illustration of wetting transition on superhydrophobic surfaces from (a) nonwetted state to (b) wetted state and schemes of enhancing the nonwetting stability against wetting transition by (c, d) increasing CA on the sidewall. (a) Nonwetted state is maintained when the surface tension can sustain the liquid pressure over the air, $P_l - P_a$. (b) Once the pressure exceeds the opposing force by surface tension, the liquid wets the sidewall of the microstructure and starts to fill the gap. The wetted surface does not transition to the nonwetted state by lowering P_l. (c) Nanostructures on the sidewall allow the CA magnified to near 180° on the sidewall. (d) A re-entrant structure allows the CA to reach the maximum value of 180° at the re-entrant corner on the sidewall.

wetting transition. Although there were several experimental studies[15−20] devoted to the fabrication of hierarchical structures, their commonly shared interests were directed to the change of static contact angle and contact angle hysteresis rather than the expanded stability of nonwetted state. In this study, we design and develop dual-scale hierarchical structures by imposing nanostructures onto two types of microstructures—posts and gratings—and investigate how the nanostructures delay the wetting transition. Our results show that the expanded stability the nanostructures provide allows for microstructures with a higher gas fraction or a larger pitch, which in turn produce increased slip lengths.

Design of Ideal Surface Structures for Large Slip

Liquid Slip. The most objective measure of how slippery a solid surface is for a liquid flowing on it is the slip length. Unlike drag reduction, for example, the slip length is unaffected by the factors not inherent to the surface such as channel geometries and flow conditions. For two model surfaces consisting of either posts[21] or grates,[22,23] analytical expressions have been derived to relate the slip length to two key surface parameters (i.e., gas fraction and structure pitch). For posts, the following expression has been reported based on the scaling law.[21]

$$\delta = L\left(\frac{a}{\sqrt{1-\phi_g}} + b\right) \quad (1)$$

where δ is the slip length, L is a pitch (the distance between centers of two adjacent gratings or posts), and ϕ_g is a gas fraction (or the area fraction of a liquid−gas interface). Also, a and b are the coefficients of the scaling law obtained by fitting numerical or experimental data to the equation. By linear fitting the results of a recent experimental study,[8] we obtain $a = 0.1555$ and $b = 0.132$.

For gratings, the following equation is available from an exact analysis.[23]

$$\delta = -\frac{L}{\pi}\ln\left[\cos\left(\frac{\pi\phi_g}{2}\right)\right] \quad (2)$$

Equations 1 and 2 indicate that the slip length increases linearly with a pitch and exponentially with a gas fraction, which has also

(15) Zhu, L.; Xiu, Y.; Xu, J.; Tamirisa, P. A.; Hess, D. W.; Wong, C.-P. *Langmuir* **2005**, *21*, 11208–11212.
(16) Li, Y.; Huang, X. J.; Heo, S. H.; Li, C. C.; Choi, Y. K.; Cai, W. P.; Cho, S. O. *Langmuir* **2007**, *23*, 2169–2174.
(17) Gao, X.; Yao, X.; Jiang, L. *Langmuir* **2007**, *23*, 4886–4891.
(18) Lee, Y.; Park, S.-H.; Kim, K.-B.; Lee, J.-K. *Adv. Mater.* **2007**, *19*, 2330–2335.
(19) Cortese, B.; D'Amone, S.; Manca, M.; Viola, I.; Cingolani, R.; Gigli, G. *Langmuir* **2008**, *24*, 2712–2718.
(20) Bhushan, B.; Koch, K.; Jung, Y. C. *Soft Matter* **2008**, *4*, 1799–1804.
(21) Ybert, C.; Barentin, C.; Cottin-Bizonne, C.; Joseph, P.; Bocquet, L. *Phys. Fluids* **2007**, *19*, 123601.
(22) Philip, J. R. *J. Appl. Math. Phys.* **1972**, *23*, 353–372.
(23) Lauga, L.; Stone, H. A. *J. Fluid Mech.* **2003**, *489*, 55–77.

been verified experimentally.[8] Note, however, the precondition for the above discussion is that the flowing liquid stays on top of the structures. In other words, the structured surface should be under a nonwetted (i.e., Cassie) state, as illustrated in Figure 1a.

Stability of Nonwetted State. In practice, a flowing liquid is usually under pressure, which encourages the liquid to fill the void in the surface structures even if their sidewalls are hydrophobic. A wetting transition or deviation from the nonwetted state, i.e., the liquid−solid contact line starting to invade the sidewall of the structures, can be predicted from a force balance between the liquid pressure and surface tension.[13] As long as the surface tension can sustain the liquid pressure, the nonwetted state illustrated in Figure 1a can be maintained. If the liquid pressure is higher than what the surface tension can sustain, however, the liquid will advance downward, leading to a fully (i.e., Wenzel) or partially wetted state illustrated in Figure 1b.

For posts, the criterion to maintain the nonwetted state is given by the following equation[13]

$$\frac{-2\gamma \cos\theta\sqrt{\pi(1-\phi_g)}}{(P_l-P_a)\phi_g L} \geq 1 \qquad (3)$$

where γ is the surface tension of liquid (72 mN/m for water at 25 °C), θ is the contact angle (CA) on the sidewall, and $(P_l - P_a)$ is the liquid pressure in reference to the air in the void. For gratings, on the other hand, the criterion to maintain the nonwetted state is given by the following equation:[13]

$$\frac{-2\gamma \cos\theta}{(P_l-P_a)\phi_g L} \geq 1 \qquad (4)$$

If the criterion for the above equations fails, the liquid will wet the sidewall, and the nonwetted state cannot be recovered easily. The above stability is more important than generally understood because the effect of deviation from the nonwetted state grows as the effective slip increases. For a giant slip over 100 μm, even a slight deviation (i.e., the liquid contact line slightly invading the sidewall) results in an unmistakable drop in the measured slip length.[24]

Ideal Structures. As the surface air fraction increases well above 90%, the main factor determining the maximum obtainable slip length turned out to be the stability of nonwetted state.[8] Equation 3 or 4 indicates one can enhance the stability by reducing a pitch L or a gas fraction ϕ_g. However, eq 1 or 2 indicates such a change will decrease the slip length, suggesting the conditions to enhance the stability and the conditions to increase the slip within a stable condition conflict with each other. As result, the slip can be maximized under a narrow optimum geometric condition requiring near-perfect samples.[8] On the other hand, eq 3 or 4 also indicates one can enhance the stability by increasing the CA θ on the sidewall, which is not in eq 1 or 2, i.e., does not affect the slip length directly. Since all the surfaces of the microstructures, including the sidewalls, in the previous studies were coated with a thin (below 100 nm) Teflon and already had a near-maximum CA θ_{smooth} (110°−120°)[25] possible on a smooth surface, as shown in Figure 1a, the only way to increase the slip length is roughening the sidewall surface to increase its own contact angle to θ_{nano}. Naturally, the scale of this additional roughness on the sidewall should be much smaller

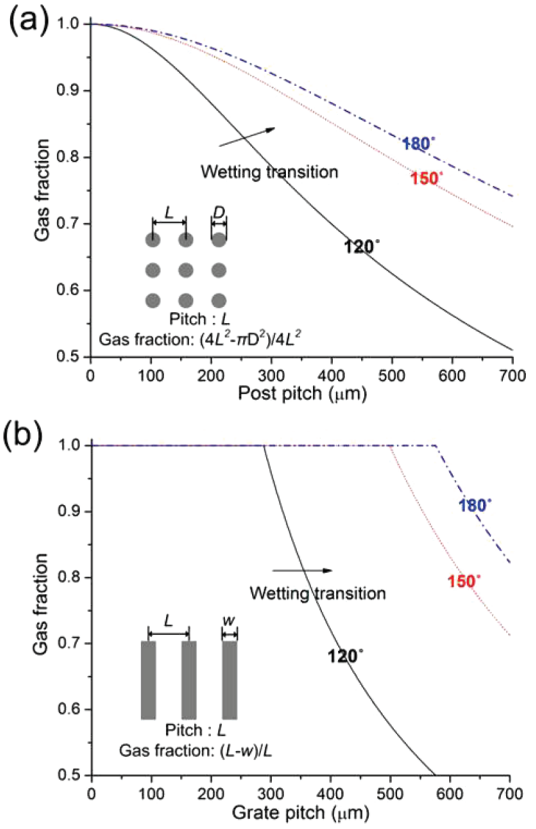

Figure 2. Theoretical wetting transition curve for (a) posts and (b) grates, quantified for a liquid pressure (over the air pressure) of 250 Pa with the effective contact angle on the sidewall as a parameter. As the contact angle increases (120° → 150° → 180°), the critical gas fraction or pitch at which a wetting transition occurs is shifted to a higher value; i.e., the range of nonwetting is expanded. A liquid flow on a lager gas fraction or a larger pitch would experience a larger effective slip as far as the nonwetted state is maintained.

(e.g., nanometers) than that of the overall surface structure that is in micrometers, as shown in Figure 1c.

As another approach, instead of changing CA θ on the sidewall surface, re-entrant structures as shown in Figure 1d can be adopted.[26] The hydrophobic re-entrant structure may allow the liquid−gas meniscus to reach a full hemispherical shape at its corner before losing the stability, which is equivalent to increasing the CA θ on the sidewall surface up to 180°. However, in our initial tests microstructures with nanostructured sidewalls exhibited a better stability against wetting transition than those with re-entrant structures. For example, on microposts of a 50 μm pitch, a nonwetted state was maintained at a 99.7% gas fraction with nanostructured sidewalls, but not with re-entrant structures. The result can be explained by the fact that the nanostructures provide a high contact angle along the sidewall while the re-entrant structures provide it only at the re-entrant corner. If any pressure surge pushes the meniscus by the re-entrant corner, an immediate and nonrecoverable wetting transition ensues.

Figure 2 shows that a wetting transition can be delayed to accommodate a higher gas fraction or a larger pitch, as the effective CA on the sidewall increases for posts (Figure 2a) and for grates (Figure 2b), quantified for the liquid pressure of 250 Pa, which is our experimental condition. For example, while the largest pitch possible before losing the nonwetted state is 285 μm

(24) Biben, T.; Joly, L. *Phys. Rev. Lett.* **2008**, *100*, 186103.
(25) Nishino, T.; Meguro, M.; Nakamae, K.; Matsushita, M.; Ueda, Y. *Langmuir* **1999**, *15*, 4321–4323.
(26) Tuteja, A.; Choi, W.; Ma, M.; Mabry, J. M.; Mazzella, S. M.; Rutledge, G. C.; McKinley, G. M.; Cohen, R. E. *Science* **2007**, *318*, 1618–1622.

for $\theta_{smooth} = 120°$ on a micropost sample with a gas fraction fixed at 0.8, it is 570 μm if $\theta_{nano} = 180°$. On a grate sample with a gas fraction of 0.9, for another example, while the largest pitch possible before losing the nonwetted state is 320 μm for $\theta_{smooth} = 120°$, it is 640 μm if $\theta_{nano} = 180°$.

Incidentally, it is worth noting here that, for a good hydrophobic surface (e.g., θ_{smooth} over 90°), the contact angle on a nanostructured surface θ_{nano} is always larger than that on a smooth surface θ_{smooth}, whether the liquid dewets or fills the nanostructures (i.e., Cassie[27] or Wenzel[28]). While the microstructure needs to be in a nonwetted state as shown in Figure 1a to allow a giant slip, the nanostructure on the sidewall does not necessarily have to be in a nonwetted state. Because the role of the nanostructures is to increase the CA on the sidewall surface so that the stability range of the nonwetted state of the microstructure is expanded, even a wetted nanostructure on the sidewall would help increase the slip length as far as θ_{nano} is larger than θ_{smooth}.

How To Make Ideal Structures. Inspired by the superhydrophobic structures observed in nature (e.g., lotus leaves), numerous fabrication schemes for hierarchical structures were developed in the past few years.[15−20] Although effective in enhancing the nonwetting stability of droplets and their rolling motions, they were unfortunately not properly designed to help enhance the effective slip of the liquids flowing on the surface. As a result, none of the hierarchical structures to date have reported any slip enhancement specifically by the secondary roughness. To meet our goal of increasing the CA on the sidewall without changing other geometries (as shown in Figure 1c), our hierarchical structures need to be constructed according to the following two design criteria. First, nanostructures should be imposed into the well-defined microstructures. In this way, geometric information needed for eqs 1−4 can be accurately estimated, facilitating a comparison of the dual-scale hierarchical structures with the equivalent single-scale microstructures. Second, nanostructures should not affect geometrical parameters other than increasing the effective CA from θ_{smooth} to θ_{nano} on the sidewall surface. Especially, the top surface of the microstructures should remain flat and smooth because any variation on the top surface would directly affect the geometric parameters (e.g., gas fraction), preventing an accurate interpretation of the eventual slip data. It should be noted that a finite slip on a nanostructured top surface, if there is any, will not help further increase the overall slip length. Since the slip length on microstructures is several orders of magnitudes larger than that on nanostructures, the influence of nanostructures on the top surfaces of the microstructures would be negligible,[21] as far as the resulting slip length is concerned. It should be noted that all the surfaces were considered hydrophobic for the above discussion. If the hierarchical structures need to be coated hydrophobic, in reality, the coating should be thin enough to keep the morphology of nanostructures intact for the purpose.

None of the reported fabrication methods satisfies both the conditions above, in particular the second. For instance, the fabrication methods seemingly satisfying the first criterion were conducted in a way that nanostructures were added onto the accurately fabricated microstructures.[15,17,20] However, this "additive" approach inevitably resulted in nanostructures covering everywhere, leading to a modification of geometric parameters of critical importance. For instance, because the nanostructure coating on the microstructure surfaces reduced the void fraction of the structures, any positive effect the coating may have on the stability would be overshadowed by the negative effect that the reduced gas fraction or pitch has on the slip length. In order to keep the key geometric parameters of the microstructure unchanged, what is desired is a "subtractive" method, which carves nanostructures into the surfaces of the microstructure, satisfying the first criterion.

While it is conceptually possible to satisfy the second criterion, e.g., masking the top surface during the etching process of roughening the sidewalls, this approach is highly dependent on the material on hand and requires the development of sophisticated micromachining techniques. In present study, where silicon is the basic material, an electrochemical etching of silicon can be considered as a good candidate to convert the silicon surface into nanostructures subtractively. It is well-known that various types of nanopores in the size ranging 2−50 nm can be generated by anodization in silicon in hydrofluoric (HF) electrolytes and their morphology can be controlled.[29] However, for the microstructures needed for an effective slip, the uniformity of nanopores over the sidewall is questionable because of a nonuniform electric field expected inside the tall and narrow microstructures. To overcome this shortcoming of the common electrochemical etching, we develop our solution by exploring two recent advances in the field of micromachining technologies. Instead of applying an external electric field, it has recently been shown that Au could be utilized as a local electrode for porous silicon etching.[30−32] It has also recently been matured that Au can be deposited on silicon by galvanic displacement deposition.[31] In essence, we deposit a thin film of Au conformally on the silicon microstructures despite their high-aspect-ratio geometry and then form uniform nanostructures into the surfaces using the conformally coated gold. This fabrication technique also allows a solution to meet the second criterion. By selectively protecting the top surface of the microstructure during the Au-assisted etching, we obtain well-defined microstructures with smooth top surfaces and roughened sidewalls, satisfying both of the design criteria described above.

Experimental Details

Fabrication. In all experiments, p-type Si (100) wafers were used. First, 1 μm thick silicon dioxide was thermally grown on as-received Si wafers, and photoresist (AZ 5214) patterns of posts or concentric grates were generated on a circular area in the diameter of 60 mm by a special photolithography technique[8] to prevent any defects on the photoresist patterns. As previously reported,[8] obtaining a near-perfect sample is of great importance in accurately quantifying the criteria for a wetting transition, since any defect can distort the experimental results by inducing an early wetting transition. In the report,[8] after identifying the main source of the defects was the airborne particles entrapped during the photoresist coating, a highly clean local environment was created just for the spin-coating step. The result was particle-free photoresist patterns and near-perfect samples. Once the photoresist patterns were verified to be free of defects, the patterns were transferred to the underlying silicon dioxide layer in an oxide etcher. Silicon substrate was subsequently carved out to form the microstructures (grates or posts) by deep reactive ion etcher (DRIE) using the silicon oxide pattern as a mask. After the wafer is cleaned by a piranha solution (H_2O_2:H_2SO_4 = 1:4) and thoroughly rinsed by deionized water, it was immersed inside 0.01 M $KAuCl_3$ (99.995% Aldrich) in a 10 wt % HF solution for 10 s to deposit gold clusters selectively onto the exposed silicon

(27) Cassie, A. B. D.; Baxter, S. *Trans. Faraday Soc.* **1944**, *40*, 546.
(28) Wenzel, R. N. *Ind. Eng. Chem.* **1936**, *28*, 988.
(29) Lehmann, V.; Stengl, R.; Luigart, A. *Mater. Sci. Eng., B* **2000**, *69−70*, 11–22.
(30) Xiu, Y.; Zhu, L.; Hess, D. W.; Wong, C. P. *Nano Lett.* **2007**, *7*, 3388–3393.
(31) Cao, L.; Price, T. P.; Weiss, M.; Gao, D. *Langmuir* **2008**, *24*, 1640–1643.
(32) Xiu, Y.; Zhang, S.; Yelundur, V.; Rohatgi, A.; Hess, D. W.; Wong, C. P. *Langmuir* **2008**, *24*, 10421–10426.

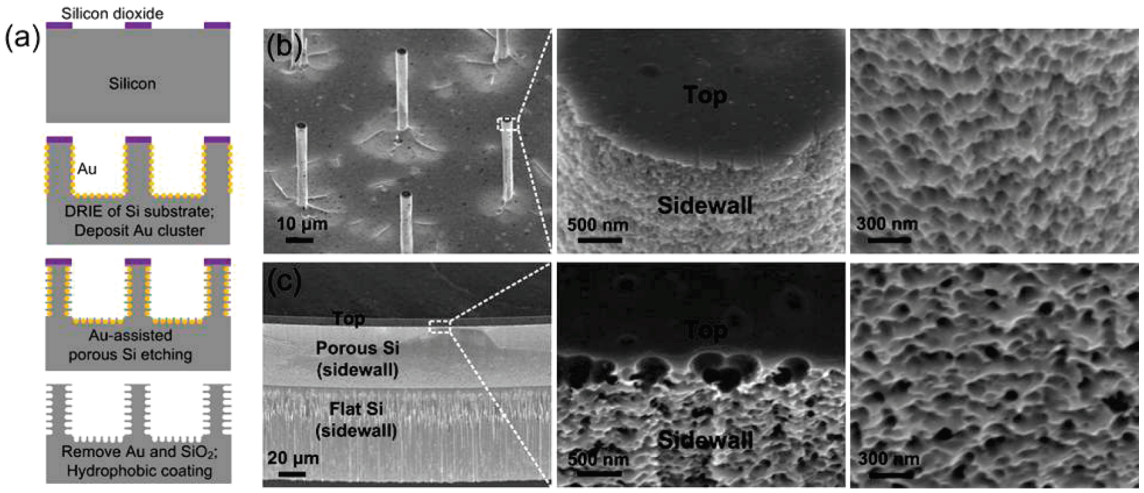

Figure 3. Fabrication process and SEM images of the micro−nano structures of Figure 1d. (a) Process flow to fabricate the dual-scale surface structures—microscale tall (50−230 μm) and thin (4−9 μm) posts or grates—with smooth top surface and rough sidewall covered with nanoscale protuberances right below the top surface. Since the protrusions are formed by etching, rather than deposition, the width of the microstructures is not compromised (i.e., the distance between posts or grates does not decrease). (b) Microposts with smooth top and nanostructured sidewall. Magnified images show nanoprotrusions. (c) A micrograte with smooth top and nanostructured sidewall. Magnified images show nanoprotrusions. Note the nanostructures cover the sidewall right below the top surface.

surface via a galvanic displacement process.[31] The silicon dioxide pattern used as a mask during DRIE remained to prevent the top surfaces from being coated with gold. Then, the wafer was placed in an etching solution ($HF:H_2O_2:H_2O$ = 1:5:10) for 30 s, where silicon is etched through a series of events of a silicon surface being oxidized by holes that are generated by the decomposition of H_2O_2 and the oxidized silicon subsequently being dissolved by HF.[32] Au clusters are believed to facilitate this oxidation and dissolution process by acting as the local electrode. As a result, after a relatively short etching (30 s in present study), nanostructures form only where Au clusters are present.[31] Finally, the remaining gold clusters and the oxide mask were removed by a gold etchant and concentrated HF solution (49 wt %).

The schematic of this fabrication process is shown in Figure 3a. After fabrication, the scanning electron microscopy (SEM) images confirmed well-defined nanostructures formed only on the sidewall with the top surface unaffected (Figure 3b). However, since the Au-assisted etching not only made the sidewall surface porous but also tended to thin the lower portion of the microstructures, the mechanical stability became a main issue for the microstructures with a high aspect ratio (e.g., 9 μm wide grates with a 230 μm height). To circumvent this problem, nanostructures were generated only on the upper part of the sidewall for the structures with a high aspect ratio (Figure 3c). In this process, Au-assisted etching was performed after a shallow etching of silicon substrate, and the substrate was additionally etched by DRIE to a sufficient depth so that the liquid−air meniscus would not touch the bottom surface. For a hydrophobic coating, we dipped the sample in H_2O_2 in order to grow a native oxide layer on the surface and treated it with 1*H*,1*H*,2*H*,2*H*-perfluorodecyltrichlorosilane (FDTS) (96%, Lancaster Synthesis, Inc.) by placing the sample in 0.1 M FDTS solution in 2,2,4-trimethylpentane (99.8%, Aldrich) under the nitrogen environment for 10 min.

Slip Measurement. The slip length on each sample was measured by a commercial rheometer (AR 2000, TA Instruments) using deionized water as a test liquid.[4,8] The cone-and-plate configuration was used in this experiment because of a constant shear rate applied over a sample. The cone had a diameter of 60 mm and an angle of 2°. The truncation between a cone and a plate was fixed at 53 μm, and the temperature was set at 25 ± 0.1 °C by a Peltier plate during the measurement. A constant shear rate in the range of 90−130 s^{-1} was imposed on the cone, and the resulting torque applied to the sample was recorded. The mathematical relation between the slip length and torque was derived in the previous study[8] on the assumption that a slip existed on the surface and was used to calculate the slip length from the measured torque in this study.

Results and Discussion

Meniscus Stability. For convenience, in this report, microstructures with all smooth surfaces are referred as micro-smooth structures, and microstructures with the smooth top surfaces and the nanostructured sidewall surfaces are referred as micro−nano structures. A contact angle θ_{nano} = 150° was obtained on hydrophobic nanostructures formed on a blank silicon surface by the fabrication processes described above. Since the nanostructuring technique and the hydrophobic SAM coating are both highly conformal in nature, it is reasonable to use the above-measured contact angle for the nanostructures formed on the sidewall of the microstructures. In comparison, the contact angle for the smooth sidewall of the microstructures was considered to be θ_{smooth} = 120°.[8]

For posts of a 50 μm fixed pitch and a liquid pressure of 250 Pa, which represent our testing conditions, the theoretical maximum gas fraction allowing the nonwetted state is drawn in Figure 4 as a function of the sidewall CA, along with the experimental data for micro-smooth structures[8] and micro−nano structures. For micro-smooth structures (i.e., sidewall CA θ_{smooth} = 120°), a nonwetted state was observed at a gas fraction as high as 99.2%, which was in good agreement with a predicted (i.e., theoretical) value of 99.1%. For micro−nano structures (i.e., sidewall CA θ_{nano} = 150°) in the present study, a nonwetted state was extended to a gas fraction as high as 99.7%, again in good agreement with a predicted (i.e., theoretical) value of 99.7%. It should be noted, however, that a further increase of sidewall CA over 150° is not so fruitful because the gain slows down so that the maximum allowable gas fraction is still below 99.8% even when the sidewall CA reaches the theoretical maximum of 180°.

Similarly, for grates of a 98% fixed gas fraction and a liquid pressure of 250 Pa, the maximum pitch allowing the nonwetted state is also presented in Figure 4. For micro-smooth structures (i.e., sidewall CA θ_{smooth} = 120°), a nonwetted state was observed at a pitch as wide as 200 μm, compared with the theoretical value of 290 μm. For micro−nano structures (i.e., sidewall

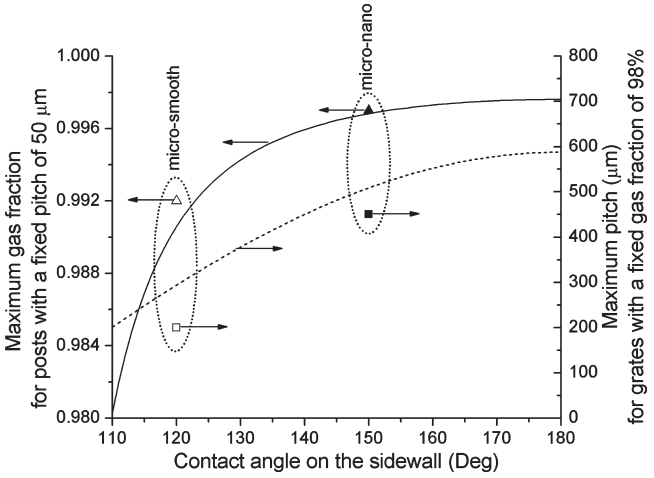

Figure 4. Maximum gas fraction of 50 μm pitch posts (triangular symbols) and maximum pitch of 98% gas fraction grates (square symbols) before wetting transition, obtained during the rheometer test (under the liquid pressure of ~250 Pa), in comparison with the theoretical transition curves. Contact angles on the smooth surface and nanostructured surface are measured to be 120° and 150°, respectively. The maximum gas fraction before wetting transition was 99.2%[8] for microposts with smooth sidewall but increased to 99.7% for microposts with nanostructured sidewall. The maximum pitch before a wetting transition was 200 μm[8] for microgrates with smooth sidewall but increased to 450 μm for microgrates with nanostructured sidewall.

CA θ_{nano} = 150°) in the present study, a nonwetted state was extended to a pitch as wide as 450 μm, compared with the theoretical value of 500 μm. The meniscus stability tests summarized in Figure 4 confirm that the force balance between the liquid pressure and surface tension explains how the wetting transition is delayed (i.e., how the stability range is extended) on micro−nano structures.

Slip Measurement. In this study, the slip length over the micro−nano structures was measured, following the established rheometric technique.[4,8,33] It was reported[4] that the slip length started to decrease with the onset of the secondary flow at the shear rate around 140 s^{-1}. In this study, we also observed such a decrease, prompting us to use the same range of 90−130 s^{-1}. Figure 5 presents the measured slip lengths on the micro−nano structures along with the previous results on micro-smooth structures[8] for comparison. In Figure 5a, which is for posts of a 50 μm pitch, a gas fraction up to 99.7% was successfully tested for micro−nano structures, producing a slip length of 120−140 μm, which is a 30−50% increase from the previous maximum (93 μm) obtained on micro-smooth structures.[8] Similarly, in Figure 5b, which is for grates of a 98% gas fraction, a pitch up to 450 μm was successfully tested for micro−nano structures, producing a slip length of 350−400 μm, which is a 100% increase from the previous maximum (185 μm) obtained on micro-smooth structures.[8] This value of 350−400 μm is by far the largest slip length ever experimentally measured with water to our knowledge.

Shear Rate. The data in Figure 5 show a shear rate dependency of slip lengths on both the posts and grates of micro−nano structures. This dependency is not evident from the data on micro-smooth structures. Although the only difference between the micro-smooth and the micro−nano structures is the presence of nanostructures on the sidewall, such a surface morphology cannot affect the amount of slip for any successful tests (i.e., nonwetting state is maintained) through air drag. One plausible

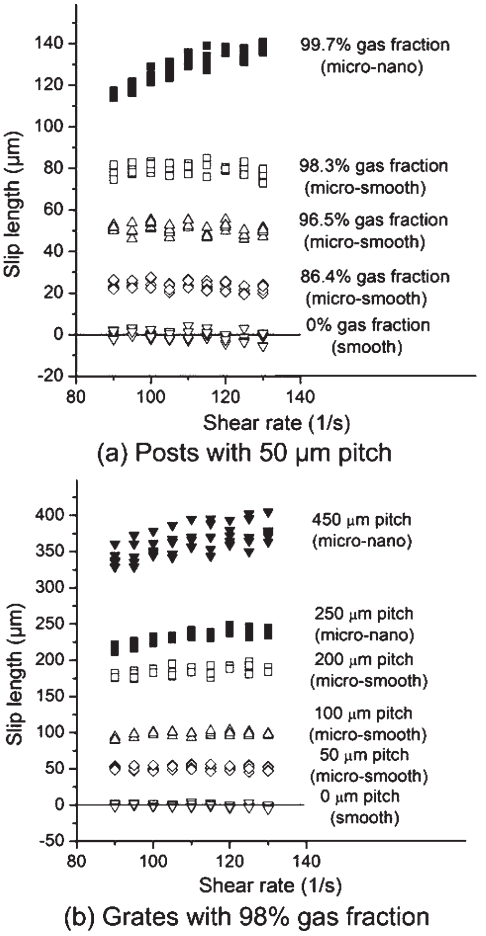

Figure 5. Slip lengths of water on (a) posts and (b) grates of micro−nano structures, measured by the rheometer, are shown with solid symbols. For a comparison, the previously reported slip lengths on micro-smooth structures[8] are included using hollow symbols. (a) Slip lengths measured on posts of 50 μm pitch and varying gas fraction. (b) Slip lengths measured on grates of 98% gas fraction and varying pitch.

explanation for the shear rate dependency is that the shear rate affects the liquid−air meniscus. A recent study[24] suggested that even a small displacement of the meniscus into the void of the microstructures could affect the slip length significantly.

One may speculate that the meniscus can be flattened by the centrifugal force at high shear rates in our rheometer test. Since the liquid−gas meniscus is allowed to bend down deeper into the micro−nano structures, which has larger stability range, than into the micro-smooth structures, the effect of meniscus flattening would be more significant for the micro−nano structure—consistent with the trend shown in Figure 5. However, our examination excluded the meniscus flatting from the possibilities, as follows. We first reasoned that any shape change of the meniscus on the microstructures should be reflected in the meniscus at the outer rim of the cone during our rheometer tests due to the conservation of liquid volume. However, calculations showed that even just a few micrometers of meniscus flattening would lead to tens of micrometers of increase in the radius of edge meniscus, which should be readily observable in our system. Since no such change was found even under a close microscope observation, we concluded the meniscus is not flattened during our rheometer tests. Another possibility is that the shear rate dependency exists for all cases but becomes more pronounced for large slips. Perhaps the micro−nano structures in this report happened to produce

(33) Choi, C.-H.; Kim, C.-J. *Phys. Rev. Lett.* **2006**, *97*, 109602.

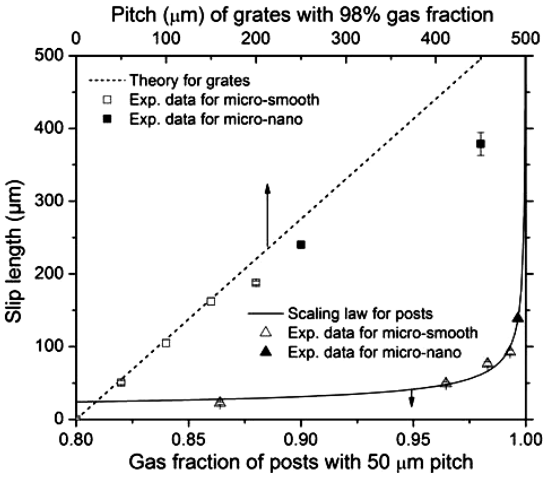

Figure 6. Slip lengths of water on posts and grates of micro−nano structures are shown with solid symbols as functions of gas fraction and grate pitch, respectively. For a comparison, theoretical values for posts and grates are drawn with a solid line and a dotted line, respectively, and the previously reported slip lengths on micro-smooth structures[8] are also included using hollow symbols. The posts have a fixed pitch of 50 μm, and the grates have a fixed gas fraction of 98%. Slip lengths increase exponentially with a gas fraction and increase linearly with a pitch.

such a large slip that the dependency is unmistakably observed for the first time. For example, the shear rate dependency of the slip length was also reported in an earlier report[4] but considered an experimental artifact such as viscous heating.

Comparison with Theory. Figure 6 compares the measured slip lengths on the micro−nano structures with theoretical values[21,23] and those obtained for micro-smooth structures in the previous study.[8] The largest of the measured slip lengths (at shear rate of 130 s^{-1}) were used for the comparison. In Figure 6a, which is for posts of a 50 μm pitch, the slip length for micro−nano structures (gas fraction of 99.7%) follows the theory[21] quite well, reinforcing the supposition that a slip length is not affected by the presence of nanostructures on the sidewall. In Figure 6b, which is for grates of 98% gas fraction, the slip length deviates lower from the theory[23] as a pitch becomes larger. There may be additional factors important for the large pitches but not accounted for in eqs 1 and 2. A recent analytical study[21] investigated how factors other than a pitch and a gas fraction—such as dissipation at a liquid−gas interface and the curvature of a liquid−gas meniscus—affected the slip length. The results showed that such additional effects could not be ignored when the slip length is expected to be very large by a large pitch or a high gas fraction. For example, for posts under the liquid pressure of 250 Pa, the slip length would be saturated at around 500 μm due to the meniscus curvature effect.[21] Although this analysis was done for an array of posts, the results could be applied to grates as well.

Conclusion

In this study, we described a hierarchical surface structure ideal to study maximal liquid slip—hydrophobic microposts or microgrates with smooth top surfaces and nanostructured sidewalls—and obtained such a micro−nano structure by developing Au-assisted porous silicon etching combined with silicon DRIE. A simple force balance between the liquid pressure and surface tension was used to explain how hydrophobic nanostructures on the sidewall would expand the stable range of the nonwetted state. The argument was corroborated by the experimental results, as micro−nano structures allowed a higher gas fraction or a larger pitch before the wetting transition than the micro-smooth structures of the same microscale surface parameters did. As a result, the measured maximum slip length on micro−nano structures was 140 μm for posts and 400 μm for grates, compared with the previously highest 93 and 185 μm on micro-smooth posts and grates, respectively. In the process, we have clarified and verified the role of the second-scale surface structure. Once the liquid is under a nonwetted state, the slip length is solely determined by the parameters of the microstructures.

It should be noted that it was important for us to generate nanostructures only on the sidewall, not only for the preservation of geometric parameters of microstructures but also for a large slip. For example, when nanostructures were generated everywhere, even by a subtractive method, we observed a significant drop in the measured slip length. We believe that the slight rounding of the top convex corners of the microstructures made by the nanostructuring process allowed a slight intrusion of the liquid−air meniscus into the void of the microstructure, decreasing the resulting slip.[24]

The maximum slip length of 400 μm in this study is the largest reported to date and is larger than the length scale of most microfluidic systems. Such a large slip length is expected to be directly relevant to even macroscopic applications. In sum, our results elucidated the role of each scale in dual-scale surface hierarchical structures in the frame of a wetting transition and a liquid slip.

Acknowledgment. This research was supported by NSF NIRT Grant No. 0103562. The authors thank Prof. P. Kavehpour for the access to the rheometer.